DMD Fast Forward. Published on March 13, 2008 as doi:10.1124/dmd.108.020644

Hydroxyitraconazole, Formed During Intestinal First-Pass Metabolism of Itraconazole, Controls the Time Course of Hepatic CYP3A Inhibition and the Bioavailability of Itraconazole in Rats

Sara K. Quinney, Raymond E. Galinsky, Vanida A. Jiyamapa-Serna, Yong Chen, Mitchell A. Hamman, Stephen D. Hall[1] and Robert E. Kimura

Division of Clinical Pharmacology, Department of Medicine, Indiana University, Indianapolis (S.K.Q., R.E.G., M.A.H., S.D.H.); Department of Industrial & Physical Pharmacy, School of Pharmacy and Pharmaceutical Sciences, Purdue University, West Lafayette, Indiana (R.E.G.); and

Section of Neonatology, Department of Pediatrics, Rush University Medical Center, Chicago, Illinois (V.A.J-S, Y.C., R.E.K.)

DMD Fast Forward. Published on March 13, 2008 as DOI: 10.1124/dmd.108.020644
This article has not been copyedited and formatted. The final version may differ from this version.

Running Title: First-Pass Formation of OH-Itraconazole and CYP3A Inhibition

Address all correspondence to:

R. E. Galinsky, Pharm.D.
Div. of Clinical Pharmacology, Rm W7123 Myers
Wishard Memorial Hospital
1001 West 10th Street
Indianapolis, IN 46202

Telephone: 317-630-8749; Fax: 317-630-8185
Email: rgalinsk@iupui.edu

Abbreviations

ITZ, itraconazole; OH-ITZ, hydroxyintraconazole; F_H, hepatic availability; LC/MS, liquid chromatography-mass spectrometry; AUC, area under the plasma concentration vs. time curve

Manuscript Details
Number of text pages: 15
Number of Tables: 0
Number of Figures: 6
Number of References: 15
Number of words in
Abstract: 236
Introduction: 413
Discussion: 1525

Abstract

Itraconazole (ITZ) is a substrate of CYP3A and both ITZ and hydroxyitraconazole (OH-ITZ), a major metabolite formed by CYP3A, are potent inhibitors of CYP3A. The concentration- and time-dependent changes in the hepatic availability (F_H) of ITZ were evaluated in rats after oral doses of 5 and 40 mg/kg. Simultaneous blood samples were obtained from the aorta, portal vein and hepatic vein for 24 hours following duodenal ITZ administration, and concentrations of ITZ and OH-ITZ determined by LC/MS. During the absorption phase, the F_H of ITZ increased from 0.2 to 1.0 reflecting the time course of hepatic CYP3A inhibition. A counter-clockwise hysteresis was observed between ITZ concentrations entering the liver ($C_{IN,ITZ}$) and F_H whereas there was no time delay observed between the change in F_H and the OH-ITZ concentrations entering the liver ($C_{IN,OH\text{-}ITZ}$). The direct relationship between $C_{IN,OH\text{-}ITZ}$ and F_H suggested that OH-ITZ was mainly responsible for the inhibition of CYP3A. A positive portal venous-aortic gradient for OH-ITZ was measured after duodenal administration of ITZ, indicating intestinal formation of OH-ITZ. The *in vivo* Ki for OH-ITZ (38 ± 3 nM) was estimated from $C_{IN,OH\text{-}ITZ}$ vs. F_H of ITZ, and is similar to values obtained from inhibition of midazolam hydroxylation in CYP3A4 supersomes (Isoherranen et al., 2004). The data suggest that OH-ITZ, formed by intestinal CYP3A, controls the time course of hepatic CYP3A inhibition and is mainly responsible for the observed increase in F_H of ITZ.

Introduction

During drug discovery and preclinical drug development, *in vivo* drug disposition and bioavailability studies are often conducted in rats, dogs, primates and other species. It is increasingly recognized that the fraction of an orally administered drug that reaches the systemic circulation is controlled by both intestinal and hepatic metabolism. However, the contribution of the intestinal epithelia to the overall "first-pass effect" of drugs is difficult to quantify because the small intestine and liver are connected in series. Correct assessment of the separate roles of hepatic and intestinal drug metabolizing capacity in determining drug bioavailability and the extent of first-pass metabolism led us to develop (Uhing and Kimura, 1995a; Uhing and Kimura, 1995b; Beno et al., 2001) and validate (Esguerra et al., 2000; Shaw et al., 2002; Uhing et al., 2004) a 5-catheter rat model for pharmacokinetic and drug-drug interaction studies in rats. Drug disposition studies can be conducted in awake, free-moving animals that have fully recovered from surgery and anesthesia and have regained their pre-operative weight. Simultaneous sampling allows us to quantify the precise time course of changes in such pharmacokinetic parameters as clearance and hepatic extraction ratio.

Itraconazole (ITZ), an orally active triazole antifungal agent, exhibits dose-dependent first-pass metabolism and nonlinear pharmacokinetics in both humans and rats (Hardin et al., 1988; Heykants et al., 1989; Yoo et al., 2000; Shin et al., 2004). Hydroxyitraconazole (OH-ITZ) is a major metabolite that is formed by CYP3A and has antifungal activity similar to ITZ (Heykants et al., 1989; Poirier and Cheymol, 1998). Both ITZ and OH-ITZ are potent inhibitors of CYP3A and OH-ITZ often displays higher plasma concentrations after ITZ administration (Heykants et al., 1989; Poirier and

Cheymol, 1998). Calculation of oral bioavailability compares the time-averaged AUC following oral administration to the time-averaged AUC after intravenous drug administration. Measurement of dose-dependence and time-dependence in bioavailability and first-pass metabolism of itraconazole may be unreliable when based upon time-average values for AUC. Using our novel, 5-catheter chronic rat model (Fig. 1), we administered ITZ intra-duodenally and obtained blood samples simultaneously from aorta, portal vein and hepatic vein. In particular, this recently validated model (Beno et al., 2001; Uhing et al., 2004) obviated the need to administer ITZ by both the intravenous and duodenal route. The measurement of the real-time changes in the absorption rate of ITZ and in hepatic availability, F_H, of ITZ and OH-ITZ, permitted us to assess the separate roles of the liver and intestine in the disposition of ITZ in rats.

Materials and Methods

Chemicals. Itraconazole (ITZ) (Sporanox® oral solution, 10 mg/mL) was obtained from Janssen Pharmaceutica (Titusville, NJ) Itraconazole (10 mg/mL) for injection and Sodium Chloride (0.9% for injection) was obtained from Abbott Laboratories (North Chicago, USA) Purified itraconazole powder was purchased from Sigma-Aldrich (St. Louis, MO). Hydroxyitraconazole (OH-ITZ) and methoxyitraconazole (MeO-ITZ) were gifts from Janssen Pharmaceuticals (Beerse, Belgium). HPLC-grade solvents and all other reagents were obtained from Fisher Scientific (Pittsburgh, PA).

Animal Preparation. Male Sprague-Dawley rats weighing 300-375 g were obtained from Charles River Laboratories, Inc. (Wilmington, MA). Rats were housed individually in standard cages and were allowed free access to rat chow and water. The environment was controlled with respect to temperature and humidity with a constant light/dark cycle. All experimental procedures conformed to the guidelines published by the National Institutes of Health and Rush University Medical Center. The Institutional Animal Care and Use Committee of Rush University approved the study.

Operative Procedures.

Operative Procedures. Rats were anesthetized with a mixture of ketamine (60 mg/kg) and xylazine (5 mg/kg) administered intramuscularly. Indwelling catheters were placed in the aorta (A), inferior vena cava (IVC), portal vein (PV), hepatic vein (HV) and duodenum (D) as shown in figure 1. Experiments were performed at least 5-7 days after surgery and anesthesia, which permits full return to preoperative physiological baseline. This chronically catheterized rat model in which multiple vascular catheters can be simultaneously sampled under non-stressed, physiological conditions has been previously

described (Uhing and Kimura, 1995a; Uhing and Kimura, 1995b) and validated (Beno et al., 2001; Uhing et al., 2004).

Experimental Design of Pharmacokinetic Studies. Animals were divided into two groups and a dose of 5 or 40 mg/kg of ITZ, was administered via the duodenal catheter. ITZ (10 mg/mL) was diluted in 0.9% sodium chloride to a final volume of 2 mL and administered over a 5-minute infusion. Aortic, portal venous and hepatic venous blood samples were simultaneously obtained at 5, 7.5, 10, 15, 20, 30, 45, 60, 120, 240, 480, 720 and 1440 min. After each blood withdrawal, animals were immediately transfused with an equal volume of blood obtained from other healthy, chronically catheterized male Sprague-Dawley rats. The red cell volume of all study animals remained stable over the time course of drug administration and blood sample withdrawal. Blood samples were stored at minus 80°C prior to assay.

Measurement of Intraconazole and Hydroxyitraconazole Concentrations. ITZ and OH-ITZ were quantified as previously described (Dennison et al., 2007). Briefly, 200 uL of ethyl acetate/hexane [50:50 v/v] and 100 uL of 5 N NaOH were added to 200 uL of serum and vortexed for 20 s. MeO-ITZ was added as an internal standard and the solution was extracted with an additional 5 ml of ethyl acetate/hexane [50:50 (v/v)]. The organic layer was evaporated at room temperature, and the residue was reconstituted in the HPLC mobile phase, 5 mM ammonium acetate/acetonitrile [20:80 (v/v)]. ITZ and OH-ITZ were separated by high performance liquid chromatograph using a C18 column (Luna, 4.6 x 150 mm, 5-µm particle size; Phenomenex, Torrance CA) at a flow rate of 1 ml/min. ITZ and OH-ITZ was quantified by mass spectrometry. LC/atmospheric pressure chemical ionization-mass spectrometry (Finnigan Navigator; Thermo Electron

Corporation, Waltham, MA) was used to monitor the following ions: *m*/*z* 721 (OH-ITZ), 705 (ITZ), and 733 (MeO-ITZ). The limit of quantitation for itraconazole and hydroxyitraconazole was 1.6 pmol/mL.

Pharmacokinetic Analysis. The hepatic availability (F_H) of a drug is the ratio of drug entering the liver that exits the liver unchanged, or $Rate_{OUT}$ / $Rate_{IN}$. The rate of ITZ entry into the liver ($Rate_{IN}$) was estimated as the sum of the amounts of ITZ entering from the portal vein and the hepatic artery, represented by the following equation:

$$Rate_{IN} = [C_{PV} \times Q_{PV} + C_A \times Q_{HA}] \quad (1)$$

Based upon microsphere studies (Richter et al., 2001) and validated by measuring the portal venous-aortic concentration gradients after superior mesenteric artery infusion of [^{14}C]-PEG in our 5-catheter rat model (Uhing et al., 2004), we assumed that portal venous blood flow (Q_{PV}) and hepatic artery flow (Q_{HA}) account for 75 and 25 percent, respectively, of total hepatic blood flow (Q_H)**.** The rate of ITZ leaving the liver ($Rate_{OUT}$) can be represented by

$$Rate_{OUT} = C_{HV} \times Q_H \quad (2)$$

Over any given time interval, typically between measurements, the average concentration (C_{AVG}) of drug can be estimated as

$$C_{AVG(t_1 \to t_2)} = \frac{AUC_{t_1 \to t_2}}{(t_2 - t_1)} \quad (3)$$

Hepatic availability (F_H) of ITZ therefore can also be estimated from:

DMD Fast Forward. Published on March 13, 2008 as DOI: 10.1124/dmd.108.020644
This article has not been copyedited and formatted. The final version may differ from this version.

$$F_H = \left[\frac{Rate_{OUT}}{Rate_{IN}}\right] = \frac{\left(\frac{AUC_{HV(t_1 \to t_2)}}{(t_2 - t_1)} \times Q_H\right)}{\left(0.75 \times Q_H \times \frac{AUC_{PV(t_1 \to t_2)}}{(t_2 - t_1)}\right) + \left(0.25 \times Q_H \times \frac{AUC_{A(t_1 \to t_2)}}{(t_2 - t_1)}\right)} \quad (4)$$

Thus,

$$F_H = \frac{AUC_{HV(t_1 \to t_2)}}{0.75 \times AUC_{PV(t_1 \to t_2)} + 0.25 \times AUC_{A(t_1 \to t_2)}} \quad (5)$$

The $C_{IN,OH\text{-}ITZ}$ vs. F_H data were fit using nonlinear regression analysis (WinNonLin®, Pharsight) and the rate constant for CYP3A inhibition (K_i) was determined using equation 6

$$F_H = \frac{Q_H}{Q_H + \frac{CL_{INT}}{(1 + \frac{I}{K_i})}} \quad (6)$$

where I is the calculated concentration of OH-ITZ entering the liver ($C_{IN,OH\text{-}ITZ}$). The calculated concentration of ITZ and OH-ITZ entering the liver represent the portal vein and hepatic artery (aortic) concentrations and differential flow rates as defined in equation 1. Hepatic blood flow was assumed to be 8-10 mL/min/100 g body weight (Uhing et al, 2004). The unbound intrinsic clearance for ITZ was 150 mL/min, estimated in other animals as the quotient of the oral clearance of ITZ and the intravenous clearance of ITZ.

Statistical Analysis: Data are expressed as mean ± S.D.

Results

Our chronically catheterized rat model is illustrated in Figure 1. Blood samples were simultaneously obtained from the aortic, portal venous and hepatic venous catheters in animals that were unrestrained. ITZ was infused over 5 minutes via the duodenal catheter at least 4-5 days after surgery and anesthesia for catheter implantation. All animals had fully recovered from the effects of anesthesia and surgery and had regained to their pre-operative weight.

The time course of itraconazole and hydroxyitraconazole concentrations entering the liver following duodenal infusion of 5 mg/kg or 40 mg/kg of itraconazole is shown in Figure 2, panel A and B, respectively. The entering concentration (C_{IN}) for drug and metabolite was estimated from an 'average' of portal venous and aortic concentrations, assuming that the liver receives 75 percent of total blood flow via the portal vein and 25 percent via the hepatic artery. ITZ was rapidly absorbed from the intestine. OH-ITZ concentrations were comparable to ITZ concentrations up to the last sampling time (1440 min). Data are shown up to 720 min.

The metabolism of ITZ to OH-ITZ via intestinal tissue was determined by subtracting the systemic concentration of drug and metabolite entering the intestine (aorta) from the concentration leaving the intestine (portal vein; Fig 3). A positive gradient indicated the net formation or production of OH-ITZ by the gut wall during ITZ absorption.

Figure 4 shows the time course of F_H of ITZ following the 5 mg/kg duodenal dose. The F_H increased from an initial value of 0.2 to 1.0 within one hour of ITZ administration (Fig 4A). The relationship between ITZ and OH-ITZ concentrations

entering the liver are shown in figure 4B. A counterclockwise hysteresis was observed. The relationship between F_H and ITZ and OH-ITZ concentrations entering the liver is shown in figure 4C and 4D, respectively. The plot of the change in F_H vs. ITZ concentration over time demonstrated a counterclockwise hysteresis consistent either with an equilibration delay between ITZ concentration and effect (F_H) or another factor controlling F_H, consistent with the production of an active metabolite. A plot of the change in F_H and OH-ITZ concentration (Fig 4D) demonstrated a direct, hyperbolic relationship. Similar relationships between F_H, ITZ and OH-ITZ were observed after the 40 mg/kg dose (Fig 5).

The relationship between F_H and OH-ITZ are shown in figure 6. An estimate of the apparent rate constant for inhibition of CYP3A was obtained by fitting the F_H vs. OH-ITZ concentration data after the two doses to equation 6.

Discussion

Dose-dependent pharmacokinetics of ITZ have been described in both rats (Yoo et al., 2000; Shin et al., 2004) and humans (Heykants et al., 1989; Templeton et al., 2007). The concentration- and time-dependent clearance and bioavailability of ITZ have been attributed to the inhibition of CYP3A by ITZ and the metabolites that are sequentially formed by CYP3A (Isoherranen et al., 2004; Templeton et al., 2007). Typically, the bioavailability of a drug is calculated from the ratio of the total AUC, from zero to infinity, following oral administration to the total AUC, following intravenous administration corrected for any differences in dose. Availability, determined in this way, represents a time-averaged parameter incorporating any changes in enzyme activity over the entire length of drug exposure. We examined the disposition of ITZ in a previously validated "5-catheter" rat model (Uhing et al., 2004). With our novel surgical model, the disposition of a drug can be characterized following either intravenous, portal venous or duodenal administration. ITZ was administered intra-duodenally and blood samples were collected simultaneously from the aorta, hepatic vein and portal vein permitting the direct measurement of drug concentration entering and exiting the liver at all sampling times. Hepatic extraction was therefore directly calculated from the difference between the rate of drug entry into and exit from the liver. F_H could be determined as the ratio of the rate of drug exiting the liver to that entering the liver. As demonstrated in this study (Figures 4A and 5A), F_H is a dynamic parameter that changes with drug concentrations entering and leaving the liver during absorption and elimination.

Changes in F_H of ITZ were out of phase with ITZ concentrations entering the liver and exhibited a counterclockwise hysteresis (Fig. 4C, 5C). F_H lagged behind the rise and

fall of ITZ concentrations during absorption and elimination. The counterclockwise nature of the hysteresis indicated that a factor other than ITZ determines the time course for the inhibition of CYP3A. The lack of hysteresis between F_H and the concentration of OH-ITZ entering the liver suggests that this metabolite or some factor with the same time-course may be a key regulator of CYP3A inhibition and, thus, the F_H of ITZ (Fig. 4D, 5D). A key finding in the present study was the observation of a positive portal venous-aortic concentration gradient of OH-ITZ (Fig 3). This indicated that this potentially important inhibitory metabolite is formed by intestinal first-pass metabolism.

ITZ is sequentially metabolized by human CYP3A4 to OH-ITZ, keto-itraconazole, and N-desalky-itraconazole (Isoherranen, 2004). ITZ and its three metabolites all inhibit midazolam hydroxylation in human liver microsomes. Similar to humans, rats also express CYP3A in both liver and intestinal tissues with higher activities being observed in the liver. Unlike humans, rats express at least four different CYP3A forms and these are selectively distributed between sexes and between the liver and intestine. Differential expression of rat CYP3A isoforms may account for the intestinal metabolism of such substrates as itraconazole but not others such as midazolam.

We quantified the time course of the change in F_H of ITZ following duodenal administration of ITZ and used the changes in F_H as a measure of CYP3A inhibition. The K_i calculated for OH-ITZ in this study was similar to that obtained from human liver microsomes (Isoherranen et al., 2004). In a recent clinical study, the time-course of exposure to the downstream metabolites was similar to that of OH-ITZ and inclusion of metabolite data improved the prediction of the magnitude of CYP3A inhibition (Templeton et al., 2007). However, the substrate affinity and inhibitory potential of OH-

ITZ for the various rat CYP3A isozymes has not been examined. As the concentrations of N-desalky-itraconazole and keto-itraconazole were not determined in this study, involvement of these metabolites in CYP3A inhibition in rats cannot be ruled out. The *Ki* value for OH-ITZ, determined *in vivo*, would also incorporate any inhibitory effects of these other, unmeasured, down-stream metabolites.

Yoo *et al.* (2000) reported that the fraction of ITZ converted to OH-ITZ in male Sprague Dawley rats following intravenous administration was 21 percent. This fraction increased to 76 percent after oral administration indicating that significant OH-ITZ formation occurs during first-pass metabolism in rats. Importantly, these investigators characterized the pharmacokinetics of OH-ITZ in rats after intravenous administration of OH-ITZ (Yoo et al., 2000). Compared to ITZ, this major metabolite had a longer half-life (10 vs. 5 hours), a smaller apparent volume of distribution (2.4 vs. 6 L/kg) and a lower systemic clearance (3.4 vs. 14.2 ml/min/kg). Similar to our results, the systemic concentrations of OH-ITZ were higher and declined more slowly compared with ITZ after oral administration of ITZ (Yoo et al., 2000). 2 hours following a 5 mg/kg duodenal dose of ITZ, we observed that the concentration of OH-ITZ entering the liver exceeded ITZ concentrations. Production of OH-ITZ by intestinal metabolism was estimated at any time-point by the concentration difference between the portal vein and the aorta. In our study, the maximal production of OH-ITZ in the gastrointestinal tract occurred within 60 minutes following duodenal administration of ITZ, similar to time course for maximal hepatic CYP3A inhibition. The time course for hepatic CYP3A inhibition may also reflect a contribution from keto-itraconazole and N-desalkyl-itraconazole, if these inhibitory metabolites are also formed from OH-ITZ by intestinal CYP3A.

Shin *et al.* (2004) reported a dose-dependent decrease in ITZ clearance in male Sprague Dawley rats. The AUC of ITZ after intragastric and intraduodenal administration was significantly smaller compared to intraportal administration suggesting substantial intestinal first-pass metabolism of ITZ in rats. However, Shin *et al.* (2004) found that the plasma concentration time course of ITZ following a 30-min intraportal infusion of 10 mg/kg was similar to that seen after intravenous infusion suggesting that little, if any, hepatic first-pass metabolism of ITZ. This stands in marked contrast to the results of Yoo *et al.* and to our results and may be attributable to the non-physiologic conditions that were present in the studies by Shin *et al.* (2004). In some ITZ disposition studies (Yoo et al., 2000; Shin et al., 2004), the drug was often administered to animals either while they were apparently under ketamine/xylazine anesthesia (Yoo et al., 2000), or up to 5-6 hours after the animals had recovered from light ether anesthesia (Shin et al., 2004). Shin *et al.* (Shin et al., 2004) reported that, possibly due to stress, many of the rats in the intestinal first-pass studies died between the 24 and 48-hour time points. We have previously shown that drug disposition studies performed within 2-3 days of anesthesia and surgery produce results that are not accurate because drug clearance and bioavailability are determined under non-physiologic conditions (Uhing et al., 2004). The acute effects of surgery and anesthesia clearly compromise hepatic CYP3A drug metabolizing activity in rats (Uhing et al., 2004). Following oral administration of 10, 30 and 50 mg/kg of ITZ (Shin et al., 2004), the mean time to the maximum plasma ITZ concentration was 158, 273 and 324 min, respectively, which is substantially longer absorption compared to our results (Fig 2A and 2B). Moreover, a 30 minute infusion of ITZ via the portal vein may have rapidly saturated

hepatic CYP3A, leading to the erroneous conclusion that rats lack hepatic first-pass metabolism of ITZ. Because pharmacokinetics of ITZ display dose- and time-dependent changes, it is crucial to eliminate other artifacts that may contribute to nonlinear drug disposition. The rats utilized in the present study were chronically catheterized and had fully recovered from effects of surgery and anesthesia, with minimal stress incurred during the study, enabling study under normal physiological conditions.

In summary, using a unique, novel 5-catheter rat model, we characterized the instantaneous hepatic availability of ITZ at multiple time points following intraduodenal administration of 5 or 40 mg/kg. Whether OH-ITZ is formed in rats by intestinal CYP3A or another rat CYP isoform remains to be directly determined. Nevertheless, we measured a positive portal venous-aortic gradient for OH-ITZ indicating that this major metabolite of ITZ is formed during intestinal first-pass metabolism in the rat. The oral bioavailability of a drug is typically calculated as the ratio of the total AUC, from zero to infinity, following oral administration to the total AUC following intravenous administration, corrected for any differences in doses. Availability, determined in this way, represents a time-averaged parameter, from zero to infinity. As demonstrated in this study (Figures 4A and 5A), availability is a dynamic parameter that can change with liver drug concentration during absorption and elimination. In the present study, the instantaneous hepatic extraction of ITZ was directly and repeatedly determined from the differences between the rate of drug entry into and exit from the liver. Hepatic availability of ITZ was used as a surrogate measure of hepatic CYP3A inhibition. An increase in hepatic availability, from approximately 0.2 to 1.0, was observed during ITZ absorption and appeared to be a function of the OH-ITZ concentration entering the liver.

The *in vivo* estimation of *Ki* is not necessarily a measure of the affinity of OH-ITZ alone for CYP3A but rather incorporates the effects of OH-ITZ and any other, unmeasured downstream metabolites on enzyme inhibition, assuming that OH-ITZ is metabolized by the same enzyme as ITZ.

References:

Beno DW, Uhing MR, Goto M, Chen Y, Jiyamapa-Serna VA and Kimura RE (2001) Endotoxin-induced reduction in biliary indocyanine green excretion rate in a chronically catheterized rat model. *Am J Physiol Gastrointest Liver Physiol* **280:**G858-865.

Dennison JB, Jones DR, Renbarger JL and Hall SD (2007) Effect of CYP3A5 expression on vincristine metabolism with human liver microsomes. *J Pharmacol Exp Ther* **321:**553-563.

Esguerra LEO, Beno DWA, Deriy L, Kimura RE and Uhing MR (2000) The effect of surgical stress on the endotoxin-induced interferon-gamma response. *Shock* **14:**561-564.

Hardin TC, Graybill JR, Fetchick R, Woestenborghs R, Rinaldi MG and Kuhn JG (1988) Pharmacokinetics of itraconazole following oral administration to normal volunteers. *Antimicrob Agents Chemother* **32:**1310-1313.

Heykants J, Van Peer A, Van de Velde V, Van Rooy P, Meuldermans W, Lavrijsen K, Woestenborghs R, Van Cutsem J and Cauwenbergh G (1989) The clinical pharmacokinetics of itraconazole: an overview. *Mycoses* **32 Suppl 1:**67-87.

Isoherranen N, Kunze KL, Allen KE, Nelson WL and Thummel KE (2004) Role of itraconazole metabolites in CYP3A4 inhibition. *Drug Metab Dispos* **32:**1121-1131.

Poirier JM and Cheymol G (1998) Optimisation of itraconazole therapy using target drug concentrations. *Clin Pharmacokinet* **35:**461-473.

Richter S, Vollmar B, Mucke I, Post S and Menger MD (2001) Hepatic arteriolo-portal venular shunting guarantees maintenance of nutritional microvascular supply in hepatic arterial buffer response of rat livers. *J Physiol* **531:**193-201.

Shaw AA, Hall SD, Franklin MR and Galinsky RE (2002) The influence of L-glutamine on the depression of hepatic cytochrome P450 activity in male rats caused by total parenteral nutrition. *Drug Metab Dispos* **30:**177-182.

Shin JH, Choi KY, Kim YC and Lee MG (2004) Dose-dependent pharmacokinetics of itraconazole after intravenous or oral administration to rats: intestinal first-pass effect. *Antimicrob Agents Chemother* **48:**1756-1762.

Templeton IE, Thummel KE, Kharasch ED, Kunze KL, Hoffer C, Nelson WL and Isoherranen N (2008) Contribution of itraconazole metabolites to inhibition of CYP3A4 *In Vivo*. *Clin Pharmacol Ther* **83**:77-85.

Uhing MR, Beno DW, Jiyamapa-Serna VA, Chen Y, Galinsky RE, Hall SD and Kimura RE (2004) The effect of anesthesia and surgery on CYP3A activity in rats. *Drug Metab Dispos* **32:**1325-1330.

Uhing MR and Kimura RE (1995a) Active transport of 3-O-methyl-glucose by the small intestine in chronically catheterized rats. *J Clin Invest* **95:**2799-2805.

Uhing MR and Kimura RE (1995b) The effect of surgical bowel manipulation and anesthesia on intestinal glucose absorption in rats. *J Clin Invest* **95:**2790-2798.

Yoo SD, Kang E, Jun H, Shin BS, Lee KC and Lee KH (2000) Absorption, first-pass metabolism, and disposition of itraconazole in rats. *Chem Pharm Bull* **48:**798-801.

Footnotes

a) This work was supported by an unrestricted grant from Pfizer.

b) Reprint requests: Raymond E. Galinsky, Division of Clinical Pharmacology, Rm W7123 Myers, Wishard Memorial Hospital, 1001 West 10th Street, Indianapolis, IN 46202

c) [1] Current Affiliation: Eli Lilly & Co., Department of Drug Disposition & Lead Optimization, Corporate Center DC0710, Indianapolis, IN 46285.

Figure legends

Figure 1. A schematic diagram of our novel, chronically catheterized rat model. The five indwelling catheters are implanted in 1) the vena cava, (2) intestine, (3) portal vein, (4) hepatic vein (5) and the aorta. ITZ was administered via duodenal catheter. Blood samples were simultaneously obtained from the aortic, portal vein and hepatic vein catheters generating the concentration vs. time profiles for ITZ and OH-ITZ.

Figure 2. Concentrations of ITZ (●) and OH-ITZ (○) entering the liver after duodenal administration of 5 mg/kg (Panel A, n = 7 rats) or 40 mg/kg (Panel B, n = 8 rats). Data are the mean + or – 1 S.D.

Figure 3. Concentration gradient of OH-ITZ across the gut wall after duodenal administration of ITZ, 5 mg/kg (○, n = 7) or 40 mg/kg (□, n = 8). Data are mean + or – 1 S.D.

Figure 4. The relationships between the time course of ITZ and OH-ITZ concentrations entering the liver and the hepatic availability of ITZ (F_H) following a single 5 mg/kg dose administered via the duodenal catheter. Panel A, Time course of F_H (●); Panel B, counter-clockwise relationship (○) between OH-ITZ and ITZ; Panel C, counter-clockwise relationship (●) between ITZ and F_H and Panel D, hyperbolic relationship (●) between OH-ITZ and F_H.

Figure 5. The relationships between the time course of ITZ and OH-ITZ concentrations entering the liver and the hepatic availability of ITZ (F_H) following a single 40 mg/kg dose administered via the duodenal catheter. Panel A, Time course of F_H (●); Panel B, counter-clockwise relationship (○) between OH-ITZ and ITZ; Panel C, counter-

clockwise relationship (●) between ITZ and F_H and Panel D, hyperbolic relationship (●) between OH-ITZ and F_H.

Figure 6. Relationship between F_H and the concentration of OH-ITZ entering the liver following either the 5 mg/kg (●) or 40 mg/kg (○) dose of ITZ as defined by equation 6. The apparent rate constant (*Ki*) for inhibition of CYP3A was 38 ± 3 nM. $R^2 = 0.33$.

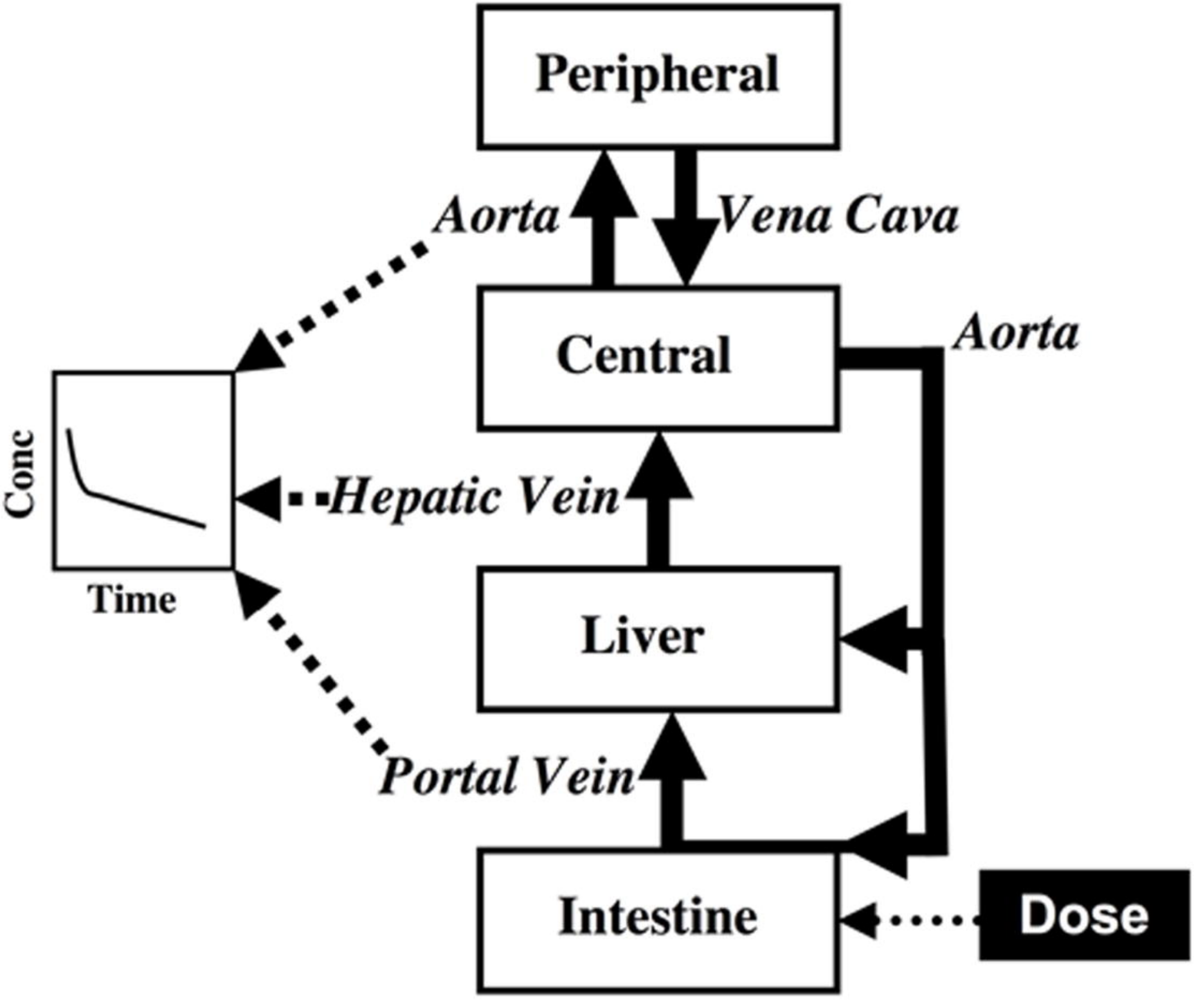
Peripheral
Aorta
Vena Cava
Central
Aorta
Conc
Time
Hepatic Vein
Liver
Portal Vein
Intestine
Dose

Figure 1

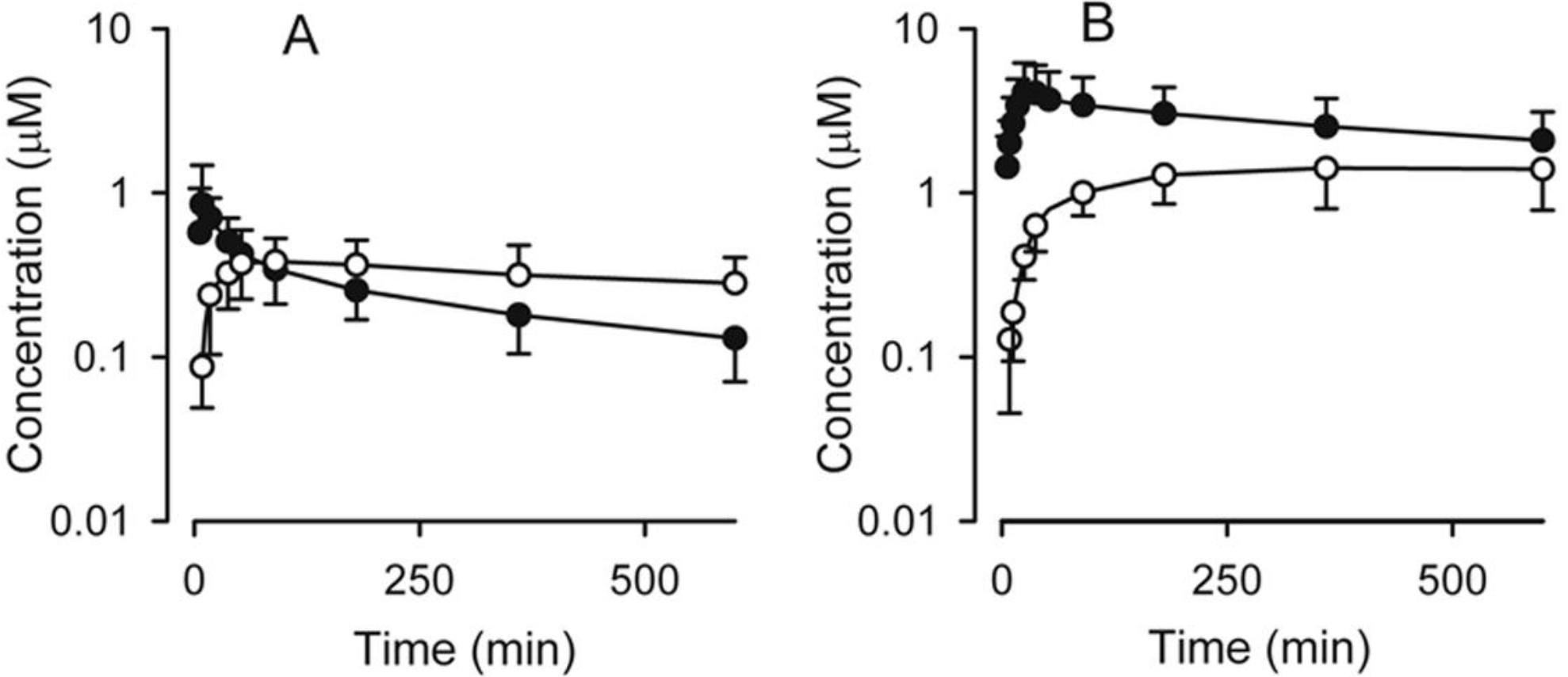

Figure 2

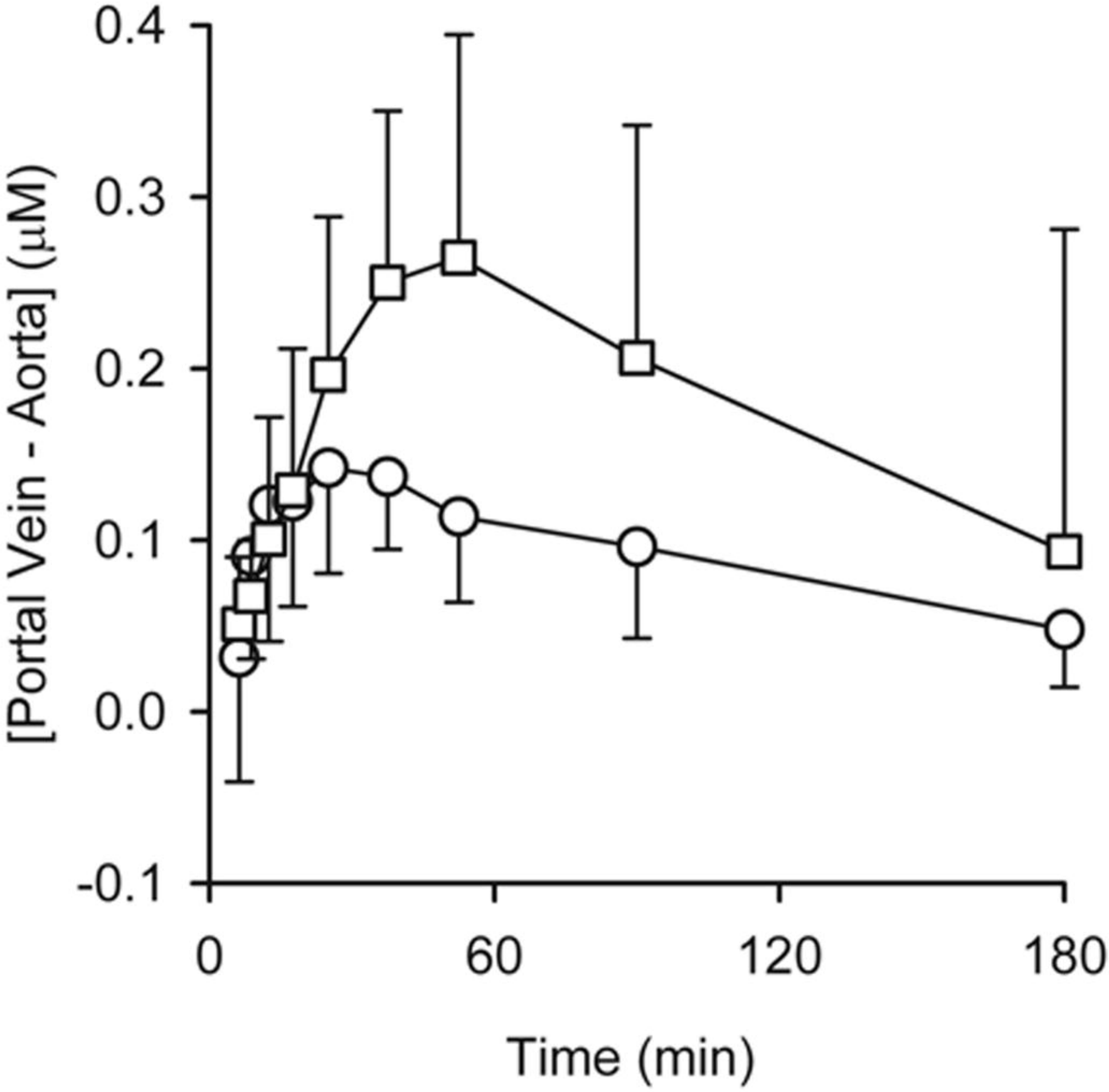

Figure 3

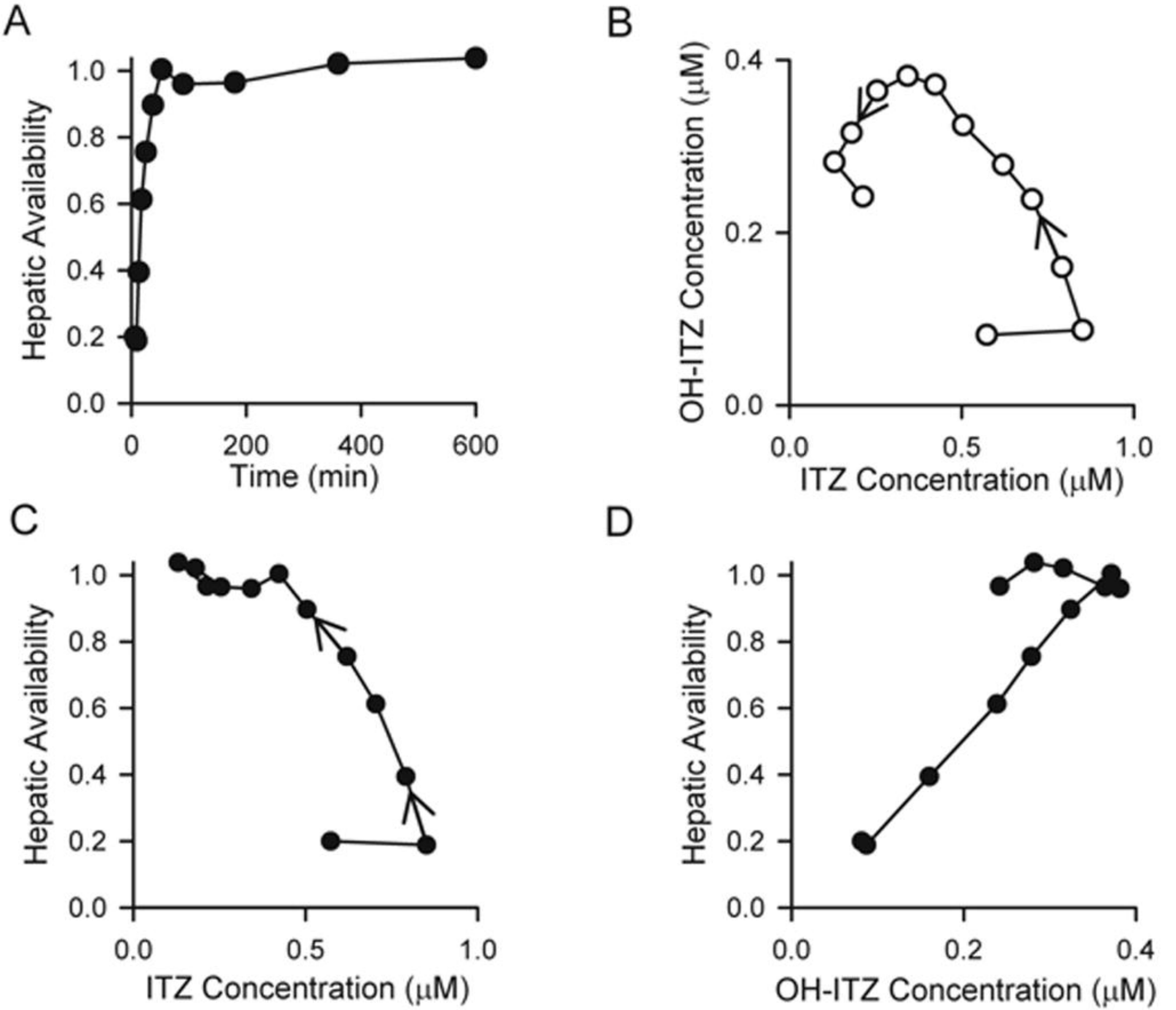
A
Hepatic Availability
1.0
0.8
0.6
0.4
0.2
0.0
0
200
400
600
Time (min)
B
OH-ITZ Concentration (μM)
0.4
0.2
0.0
0.0
0.5
1.0
ITZ Concentration (μM)
C
Hepatic Availability
1.0
0.8
0.6
0.4
0.2
0.0
0.0
0.5
1.0
ITZ Concentration (μM)
D
Hepatic Availability
1.0
0.8
0.6
0.4
0.2
0.0
0.0
0.2
0.4
OH-ITZ Concentration (μM)

Figure 4

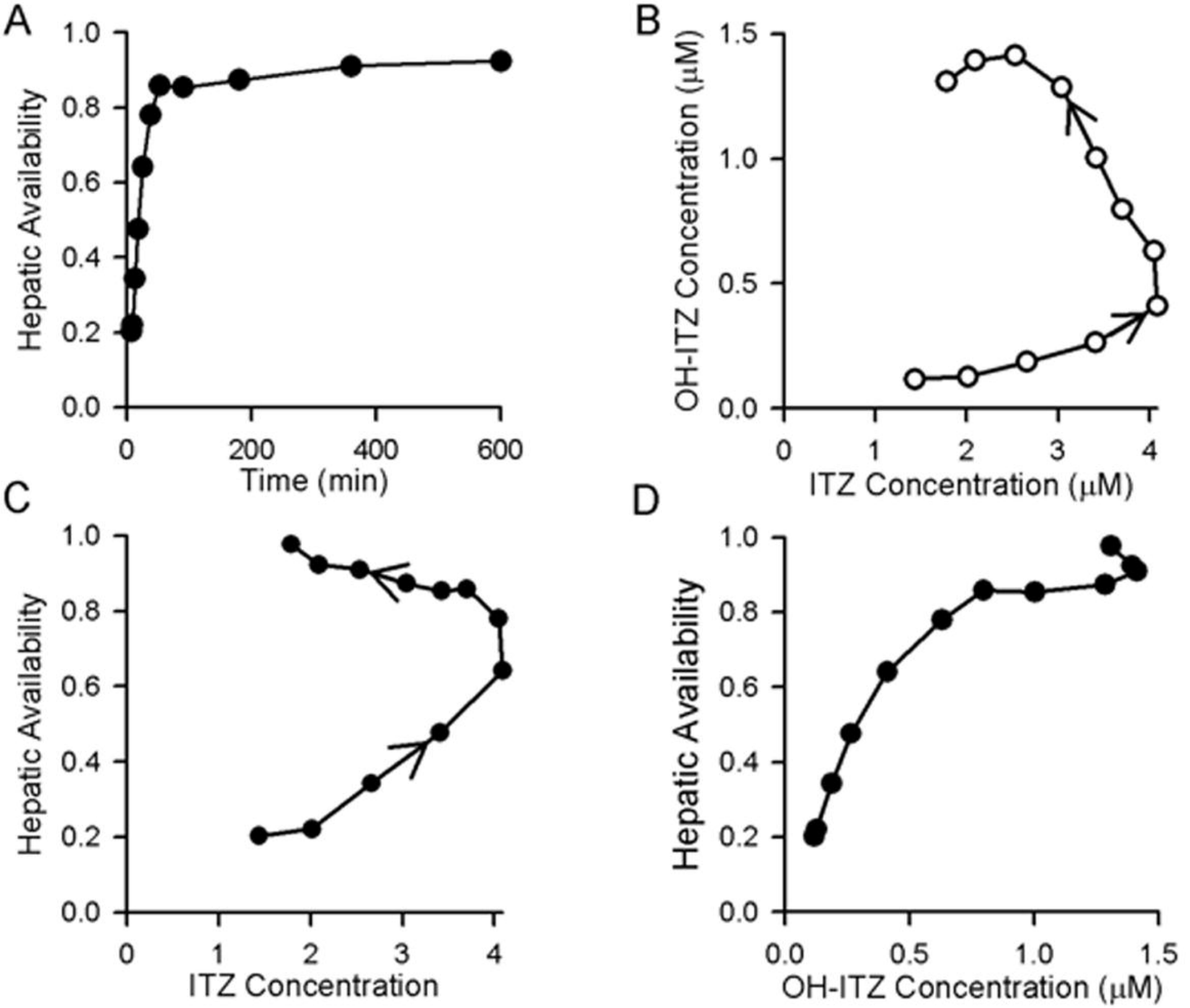
A
Hepatic Availability
1.0
0.8
0.6
0.4
0.2
0.0
0
200
400
600
Time (min)
B
OH-ITZ Concentration (μM)
1.5
1.0
0.5
0.0
0
1
2
3
4
ITZ Concentration (μM)
C
Hepatic Availability
1.0
0.8
0.6
0.4
0.2
0.0
0
1
2
3
4
ITZ Concentration
D
Hepatic Availability
1.0
0.8
0.6
0.4
0.2
0.0
0.0
0.5
1.0
1.5
OH-ITZ Concentration (μM)

Figure 5

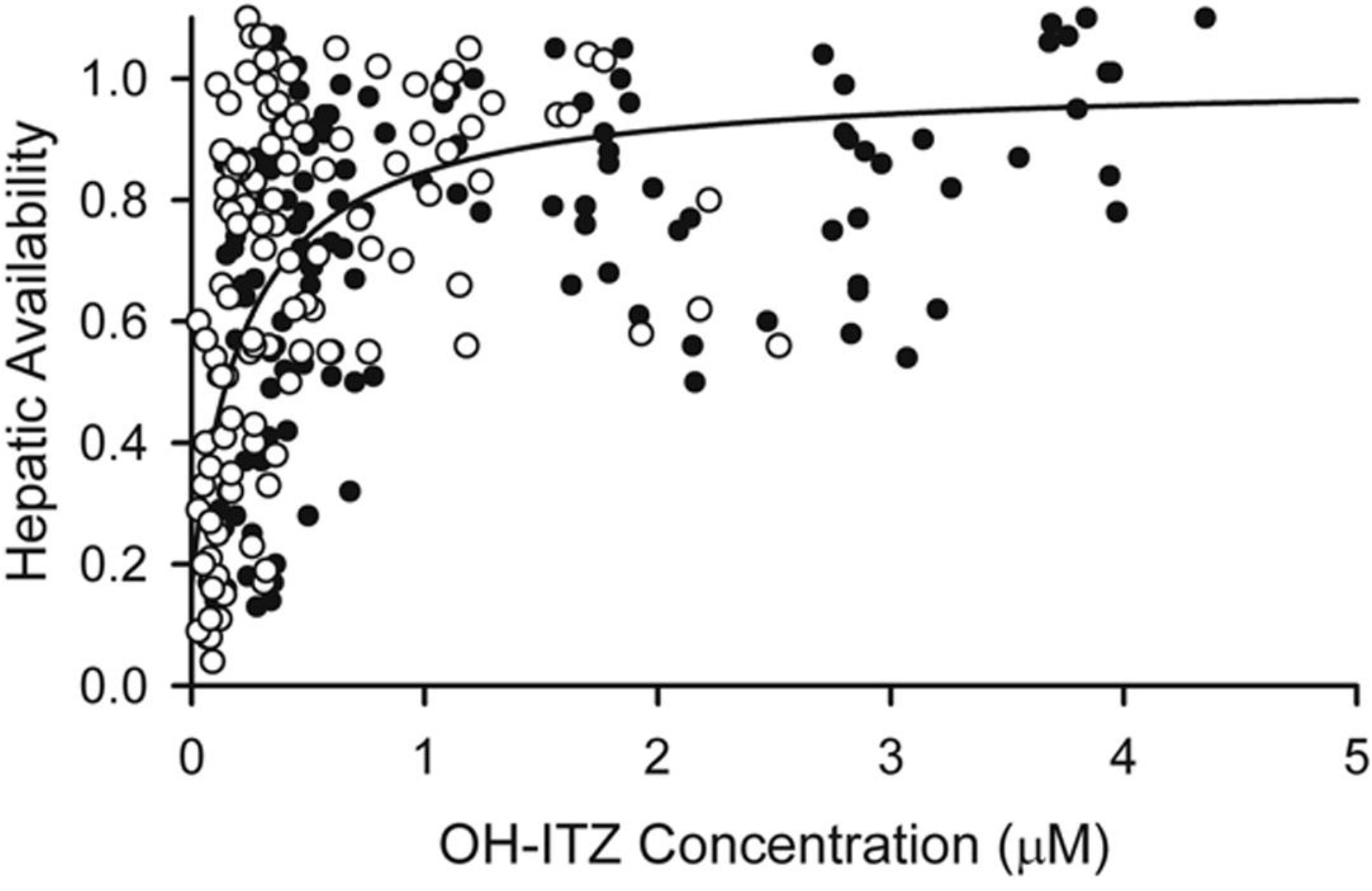
Hepatic Availability
1.0
0.8
0.6
0.4
0.2
0.0
0
1
2
3
4
5
OH-ITZ Concentration (μM)

Figure 6